Influence of hydrogen on the magnetic properties of iron-rich metallic glasses (invited)

J. M. D. Coey, D. H. Ryan, and Yu Boliang
Department of Pure and Applied Physics, Trinity College, Dublin 2, Ireland

Melt spun and sputtered amorphous alloys from the *a* $Fe_x M_{100-x}$ series with M = Y or Zr can be electrolytically hydrogenated up to a maximum of about 3 hydrogens per M, while retaining their mechanical integrity. Hydrogen uptake has been monitored *in situ* during hydrogenation by following the increase in length of the melt-spun ribbons. Values of up to 7% have been found, and the corresponding increase in volume per absorbed hydrogen is approximately 0.5 Å^3. Hydrogen diffusion constants have been estimated from the mechanical relaxation, and activation energies of order 0.4 eV have been deduced. The binding energy is about 1 eV per hydrogen. Desorption at elevated temperatures preceeds crystallization of the alloys studied, and the hydrogen-loaded materials retain much of their charge at room temperature for periods of order one year. Iron-rich yttrium alloys have a moment close to 2 μ_B/Fe, but they are asperomagnets, the iron moments freezing in a random noncollinear arrangement which possesses a net moment, below their spin freezing temperature of about 100 K. On hydrogenation they become excellent soft ferromagnets with a Curie point at 400–500 K, although there is little change in the magnitude of the iron moment. The effect is attributed to a shift in the exchange distribution towards more positive values on dilation of the interatomic spacings. Iron-rich zirconium alloys are quite different. They are essentially weak itinerant ferromagnets with a greatly reduced iron moment, and pure amorphous iron, judging from *a* $Fe_x M_{100-x}$ as $x \rightarrow 100$, would be nonmagnetic. On hydrogenation however they tend towards the same ferromagnetic state as the hydrogenated yttrium alloys.

PACS numbers: 75.50.Kj, 81.40.Rs, 76.80. + y

I. INTRODUCTION

A significant body of work has been done on crystalline metal-hydrogen systems,[1] including intermetallic compounds of an early transition element from the IIIa, IVa, or Va subgroups (including rare earths) with a late transition element from subgroup VIIIa. Examples are $LaNi_5$ and TiFe. The early transition element is mainly responsible for the hydrogen absorption capacity, and the principal effects of hydrogen are to dilate the lattice and modify the band structure, especially in the region 5–7 eV below the Fermi energy.[2] Changes in interatomic distance and electronic structure naturally have consequences for the magnetic properties of the intermetallic compounds. We restrict our attention here to iron alloys. Zero temperature magnetization or ^{57}Fe hyperfine field of $ScFe_2$, YFe_2, YFe_3, Y_6Fe_{23}, $CeFe_2$, and $HoFe_2$ all increase on hydrogenation.[3–5] For example, the moment per iron μ_{Fe} passes from 1.46 μ_B in YF_2 to 1.83 μ_B in YFe_2H_4. Curie temperature changes do not necessarily follow the change in iron moment. T_C decreases in YFe_2, is unchanged in YFe_3, and increases Y_6Fe_{23} or $CeFe_2$.[4] In each case the effect of hydrogen is opposite to that of pressure, which suggests that the dependence of exchange interactions on interatomic spacing is the principal factor determining T_C of three iron-rich intermetallic compounds.

Turning now to noncrystalline iron-based alloys, some trends may be discerned from the mass of magnetic data on iron-metal and iron-metalloid amorphous alloys *a* $Fe_x M_{100-x}$.[6] There is a critical concentration, typically around $x = 40$, where moments first appear on the iron. The average iron moment and Curie temperature for the ferromagnetic systems then increase with increasing x. However in some cases, notably *a* $Fe_x B_{100-x}$ (Ref. 7) and *a* $Fe_x Zr_{100-x}$,[8,9] these quantities pass through a maximum, and then decline as $x \rightarrow 100$. Other systems, notably sputtered *a* $Fe_x Y_{100-x}$ (Ref. 10) are not ferromagnetic for any value of x because of a broad distribution of mainly ferromagnetic exchange with some antiferromagnetic interactions which leads to asperomagnetic order. All these results have led to speculation about the magnetic state of pure amorphous iron. Possibilities which can be justified by extrapolating different alloy systems to $x = 100$ are: (i) a ferromagnet with moment $\langle \mu_{Fe} \rangle \gtrsim 2\mu_B$, similar to bcc iron, or fcc iron extrapolated from alloys with a large lattice parameter[11]; (ii) a noncollinear random magnet with competing ferromagnetic and antiferromagnetic interactions, also with $\langle \mu_{Fe} \rangle > 2\mu_B$; (iii) a weak itinerant ferromagnet with greatly

 0021-8979/84/061800-05$02.40

reduced iron moment $\langle \mu_{Fe} \rangle \simeq 1 \mu_B$.[12] Possibility (ii) is supported by data on $a\text{Fe}_x\text{Y}_{100-x}$.[10] Possibility (iii) receives support from studies of amorphous $\text{Fe}_x\text{Zr}_{100-x}$ alloys with $x \simeq 90$, which show many of the magnetic properties usually associated with weak itinerant ferromagnets.[9,13,14]

In principle, the addition of hydrogen to an amorphous magnetic alloy allows the band structure and the exchange interactions to be modified in a controllable way. Fujimori *et al.* were the first to report significant increase in $\langle \mu_{Fe} \rangle$ and T_C for $a\text{Fe}_x\text{Zr}_{100-x}$ with $x = 91$ or 92 on hydrogenation.[15] We have previously described a nearly fourfold increase in the magnetic ordering temperature of $a\text{Fe}_{88}\text{Y}_{12}$ (Ref. 16) and changes in magnetic structure of $a\text{Fe}_{89}\text{Zr}_{11}$ (Ref. 17) induced by hydrogen. There have also been some other preliminary reports on hydrogen in rare-earth amorphous alloys.[18] The aim of the present paper is to describe hydrogen loading of Fe-Zr and Fe-Y amorphous alloys in some detail, and to discuss its effects on the magnetic state of these materials.

II. HYDROGENATION OF AMORPHOUS ALLOYS

Three series of amorphous materials have been investigated; melt-spun ribbons of Fe-Zr with $88 \leqslant x \leqslant 93$, melt spun ribbons of Fe-Y with $25 \leqslant x \leqslant 50$ and sputtered thick films of Fe-Y with $75 \leqslant x \leqslant 88$. The ribbons were prepared by Z. Altounian and the foils by A. Liénard.

An electrolytic hydrogenation procedure was used where the sample forms the cathode of a cell with a platinum anode. The electrolyte was $0.1M$ K_2CO_3 containing 10 ppm of sodium arsenite. Current densities of order 1 mA/mm^2 of sample were used. Acid electrolytes proved very corrosive for certain alloy compositions, allowing them to hydrogenate directly without passing any current.[19]

A convenient way of following hydrogen uptake in melt-spun ribbons is by monitoring their increase in length. With an optical lever arrangement and a low-power laser, variations of 15 μm were detectable in the length of a 4–5 cm ribbon maintained under slight tension. Some results for

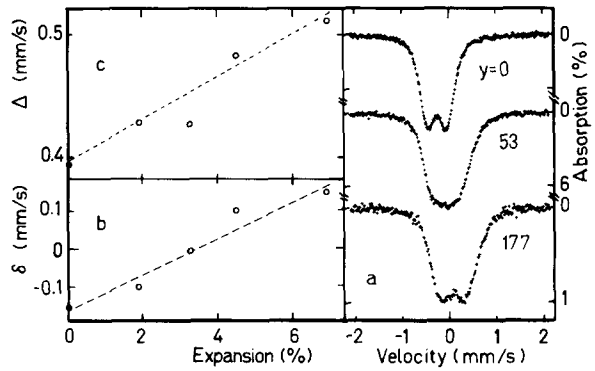

FIG. 2. (a) Mössbauer spectra of $\text{Fe}_{40}\text{Y}_{60}\text{H}_y$ at room temperature for different hydrogen loading. (b) Isomer shift and (c) quadrupole splitting as a function of y.

$\Delta l(t)$ are given on Fig. 1. There is usually a short activation time, followed by a period of rapid expansion and then a slow approach to saturation. Small additional increases of length could be achieved by increasing the current density. Assuming isotropic expansion, volume increases of up to 23% were achieved with no sign of the sample disintegrating, but 5%–10% was more usual. Whereas aFe-Y alloys became brittle, and tended to break on removing them from the cell, the aFe-Zr alloys did not, and could be handled freely without breaking.

X-ray diffraction was performed on selected samples and Mössbauer spectra were taken of them all. No sign was found of crystallization nor of any stable two-phase mixture produced by hydrogenation. Instead, the spectra changed continuously with increasing hydrogen content, as illustrated in Fig. 2. Some insight into the long term stability of amorphous hydrides is provided by the three spectra of $a\text{Fe}_{88}\text{Y}_{12}$ in Fig. 3. The effect of hydrogen on this alloy is to raise its magnetic ordering temperature well above room temperature. Shortly after loading, the hydrogen has diffused throughout the sample which then appears uniformly ferromagnetic. The hydrogenated alloy then retains its ferro-

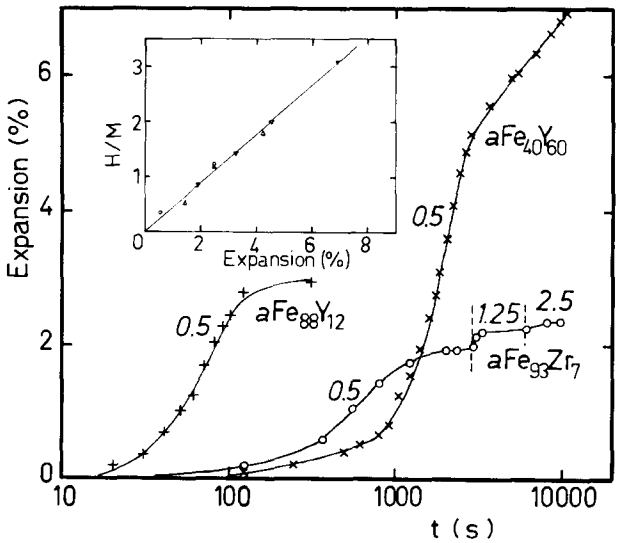

FIG. 1. Length change as a function of charging time for melt spun ribbons. The figures indicate the current in mA/mm^2. Inset: Hydrogen content as a function of expansion for $\text{Fe}_{40}\text{Y}_{60}$(▽), $\text{Fe}_{88}\text{Y}_{12}$ (○).

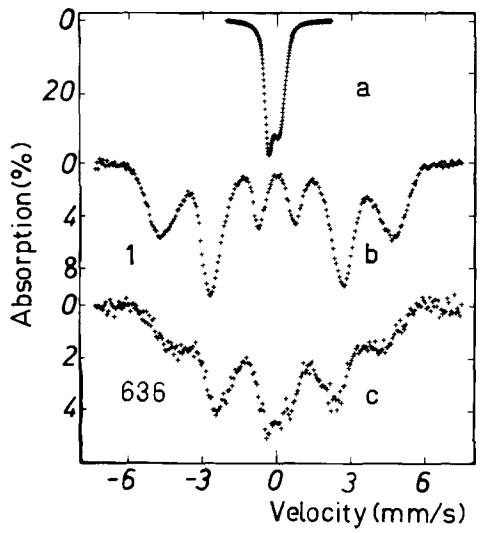

FIG. 3. Mössbauer spectra of $\text{Fe}_{88}\text{Y}_{12}$ (a) before and (b)–(c) after hydrogenation. Times shown are the times (in days) elapsed since hydrogenation was completed.

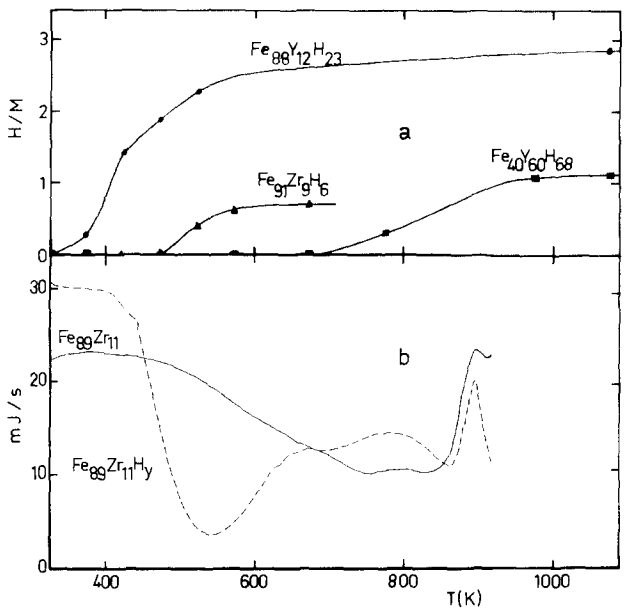

FIG. 4. (a) Hydrogen evolution as a function of baking temperature for hydrogenated amorphous alloys. (b) Differential scanning calorimeter traces for $a\text{Fe}_{89}\text{Zr}_{11}$ before hydrogenation (solid line) and after hydrogenation (dashed line).

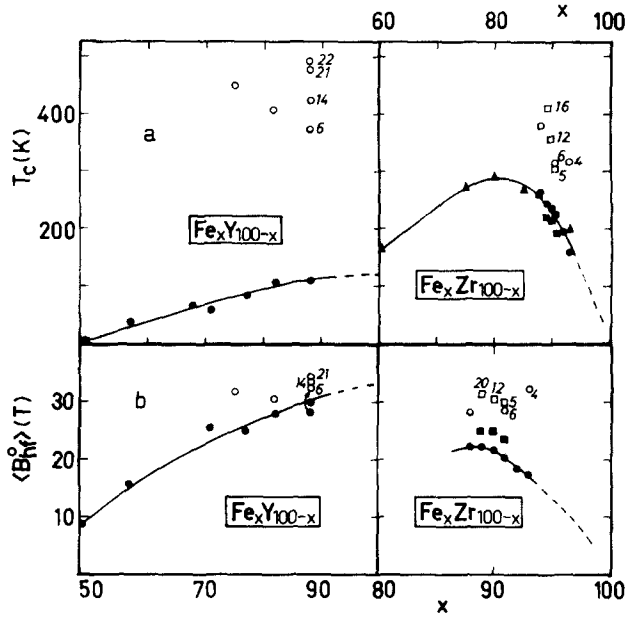

FIG. 6.. Composition dependence of (a) magnetic ordering temperature and (b) average zero temperature hyperfine field for $a\text{Fe}_x\text{M}_{100-x}$. Data on hydrogenated alloys $a\text{Fe}_x\text{M}_{100-x}\text{H}_y$ are indicated by open symbols together with the value of y.

magnetism for periods of at least two years. Some decrease in hyperfine field with time reflects very slow hydrogen loss and possibly also structural relaxation. Laboratory measurements can therefore be made on the alloys without fear that they are going to evolve significantly after the short preliminary period needed for the hydrogen to distribute itself uniformly throughout the bulk. Initial entry of hydrogen at the surfaces of the foils and ribbons during electrolysis causes them to crinkle and coil up, respectively. Ribbons absorb hydrogen preferentially through the lower, dull surface but they subsequently uncoil as hydrogen diffuses across thickness. The timescale of this behavior can be used to provide a rough estimate of the diffusion constant; values of D of $1.32 \pm 0.4 \times 10^{-14}\text{m}^2/\text{s}$ and $2.87 \pm 0.7 \times 10^{-3}\text{m}^2/\text{s}$ were deduced for $\text{Fe}_{89}\text{Zr}_{11}$ and $\text{Fe}_{40}\text{Y}_{60}$, respectively. Assuming thermally-activated diffusion $D = D_0 e^{-E_a/kT}$ with prefactor $D_0 = 3 \times 10^{-7}\text{m}^2\,\text{s}$,[20] an activation energy E_a of approximately 0.4 eV is obtained.

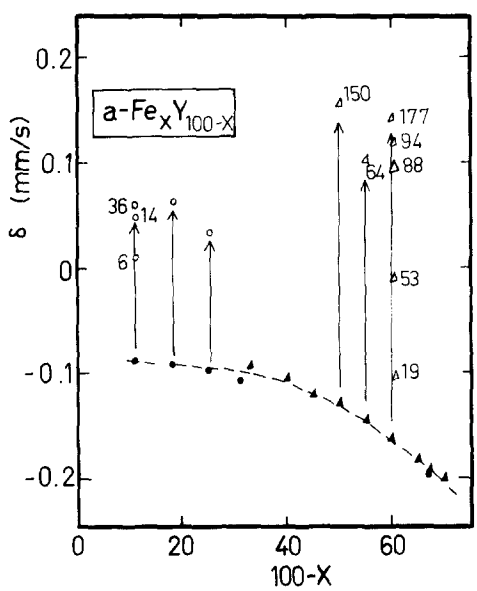

FIG. 5. Isomer shift (relative to metallic iron) of $a\text{Fe}_x\text{Y}_{100-x}\text{H}_y$ alloys. $y = 0$ (●▲); $y \neq 0$ (○△ with values shown).

The thermal stability and hydrogen content of the amorphous hydrogen-loaded alloys were investigated by slowly heating them up to 1300 K in a miniature quartz tube attached to an oil manometer, thereby monitoring hydrogen evolved as a function of temperature. Typical data are shown on Fig. 4(a), Fig. 4(b) compares DSC traces for hydrogenated and unhydrogenated $a\text{Fe}_{91}\text{Zr}_{11}$. The broad endothermic feature corresponds to hydrogen evolution, which is essentially complete before crystallization occurs at 900 K. The enthalpy absorbed is equivalent to a binding energy of approximately 1 eV per hydrogen atom.

The relationship between dilation and hydrogen content, included in Fig. 1, is approximately linear and independent of composition when H per M is plotted. There is an added volume of about 0.5 Å^3 per hydrogen. ^{57}Fe isomer shifts (Fig. 5) provide indirect evidence of a hydrogen-induced modification in electronic structure. Changes on hydrogenation indicate a decreased electron density at the nucleus, but the effect, for $\text{Fe}_{88}\text{Y}_{12}$, $(\partial\delta/\partial \ln V) \sim 2.5$ mm/s, is about twice as great as expected from the normal volume dependence.[21] For $\text{Fe}_{40}\text{Y}_{60}$, however, the change might be accounted for by the change of volume alone.

III. MAGNETIC PROPERTIES

A. $a\text{Fe}_x\text{Y}_{100-x}$

Figure 6(a) shows the composition dependence of the spin freezing temperature for asperomagnetic $a\text{Fe}_x\text{Y}_{100-x}$, marked by the peak in the low-field susceptibility. A considerable degree of short-range order with fluctuating, partly

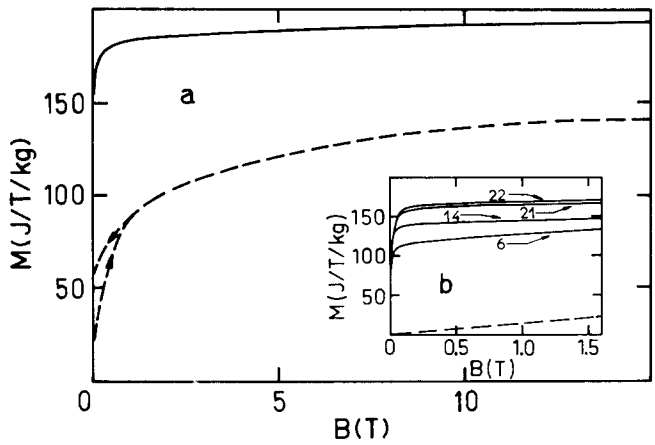

FIG. 7. Magnetization curves of (a) $a\mathrm{Fe}_{88}\mathrm{Y}_{12}$ before and after hydrogenation at 4.2 K and (b) magnetization curves of $a\mathrm{Fe}_{88}\mathrm{Y}_{12}\mathrm{H}_y$ with value of y shown at 296 K.

ferromagnetic character persists to much higher temperatures.[10] Figure 7 illustrates some magnetization curves of $a\mathrm{Fe}_{88}\mathrm{Y}_{12}$. Initially the alloy had a spin freezing temperature of 109 K. It is strongly paramagnetic at room temperature, and impossible to saturate at 4.2 K even in fields of 15 T. Average Mössbauer hyperfine fields extrapolated to zero temperature are shown in Fig. 6(b). For this composition $\langle B^0_{\mathrm{hf}}\rangle = 30.1$ T, which corresponds to an atomic moment $\langle \mu_{\mathrm{Fe}}\rangle \simeq 2\mu_B$, but Mossbauer spectra in large applied fields clearly indicate that the moments are not aligned in a collinear configuration.[10] On hydrogenation, the iron-rich alloys become excellent soft ferromagnets. The spontaneous magnetization of $a\mathrm{Fe}_{88}\mathrm{Y}_{12}\mathrm{H}_{36}$ is easily saturated below its Curie temperature $T_C = 410$ K and the room temperature coercivity is only 40 μT (0.4 Oe). However there is little change in the hyperfine field; $\langle B^0_{\mathrm{hf}}\rangle$ only increases to 32.5 T.[16] Data for another sample over a range of hydrogen content is included on Fig. 6(b).

Very little is needed to turn the iron-rich alloys ferromagnetic; for example, $T_C = 350$ K for $a\mathrm{Fe}_{88}\mathrm{Y}_{12}\mathrm{H}_y$ when $y = 6$. However, the magnetic properties do seem to evolve *continuously* towards collinear ferromagnetism with increasing y, and the magnetization curves in Fig. 7 indicate an increased spontaneous magnetization and reduced high-field slope as the hydrogen content increases.

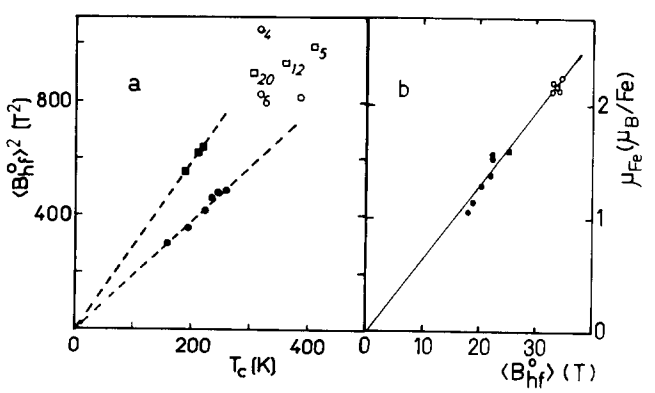

FIG. 8. (a) Plot of mean square hyperfine field as a function of Curie temperature for $a\mathrm{Fe}_x\mathrm{Zr}_{100-x}\mathrm{H}_y$. $y = 0$: solid symbols; $y \neq 0$: open symbols (value of y shown). (b) Plot of average iron moment at 4.2 K against average hyperfine field of ferromagnetic $a\mathrm{Fe}_x\mathrm{M}_{100-x}$.

B. $a\mathrm{Fe}_x\mathrm{Zr}_{100-x}$

A common feature of the magnetic properties of iron-rich $a\mathrm{Fe}_x\mathrm{Zr}_{100-x}$ and $a\mathrm{Fe}_x\mathrm{Y}_{100-x}$ is that they are extremely sensitive to preparation conditions. We examined two sets of Fe-Zr ribbons, one with $x = 89$, 90, and 91, the other with $x = 88$, 89, 90, 91, 92, and 93. A preliminary report on $a\mathrm{Fe}_{89}\mathrm{Zr}_{11}$ from the first set has appeared elsewhere.[17] Figure 6(a) shows that there is a maximum in the Curie temperature near $x = 80$, followed by a sharp decline as $x \rightarrow 100$. There is a corresponding decline in $\langle B^0_{\mathrm{hf}}\rangle$. The relation between $\langle \mu_{\mathrm{Fe}}\rangle$ and $\langle B^0_{\mathrm{hf}}\rangle$ is linear with a slope of 15.5 T/μ_B [Fig. 8(b)]. Hyperfine field can therefore be taken to be proportional to iron moment. Figure 8(a) is a plot of $\langle B^0_{\mathrm{hf}}\rangle^2$ against T_C. The two sets of samples are clearly distinguished, but the points for each set fall on a straight line through the origin, $T_C \propto \langle \mu_{\mathrm{Fe}}\rangle^2$, as expected from the theory of itinerant ferromagnetism with a constant exchange interaction. The first set have larger moments but lower Curie temperatures than the second, so it appears that the preparation procedure influences the exchange. Furthermore, on hydrogenation the points in Fig. 8(a) do not generally lie on the same straight line as the point for the unhydrogenated alloy, so hydrogenation may either increase or decrease the average exchange interactions, besides increasing the moment. That hydrogen does more than simply act as a negative pressure in increasing the Curie temperature of $a\mathrm{Fe}_x\mathrm{Zr}_{100-x}$ is evident from comparison of the volume dependence of T_C in the two cases. The pressure dependence of T_C in iron-rich $a\mathrm{Fe}_x\mathrm{Zr}_{100-x}$ (Ref. 9) is $\partial T_C/\partial P = -6\times10^{-8}$ km^2/N. Taking the bulk modulus of $a\mathrm{Cu}_{60}\mathrm{Zr}_{40}$, 7×10^{-12} m^2/N,[22] as representative of the iron alloys, we find $\partial T_C/\partial(\ln V) = 8600$ K. Values found by hydrogenation are in the range 1500–6000 K.

There have been several reports of spin glass behavior in iron-rich aFe-Zr alloys at low temperatures.[14,23,24] While much of the published magnetic data may be explained by the appearance of some coercivity in the ferromagnetic phase below about 100 K, we have nevertheless observed a large reduction in spontaneous magnetization below 80 K for the $x = 11$ sample (first set) which is unrelated to coercivity.[17] Apparently there is a transition from a ferromagnetic state to an asperomagnetic one with about half the spontaneous magnetization at $T = 0$. No such transition was observed in the second set of alloys.

IV. DISCUSSION

There is evidently a real difference between the magnetic states of iron-rich aFe-Zr and aFe-Y. In the zirconium alloys, the iron moment becomes progressively weaker as Zr content decreases. Extrapolation from the iron-rich compositions leads us to believe that in the zirconium-free limit pure amorphous iron would actually be nonmagnetic, like the hcp phase of crystalline iron.[25]

Kaul[14] has suggested that many of the properties of

iron-rich zirconium alloys may be explained by the theory of weak itinerant ferromagnetism, but that there are also localized electrons present with antiferromagnetic interactions responsible for the "spin glass" behavior.

The picture which emerges from the iron-rich yttrium system is quite different. There the iron possesses its normal moment of around $2\mu_B$, but a distribution of positive and negative exchange interactions ensures that the iron ground state is not a collinear ferromagnetic but an asperomagnetic configuration. A similar result would be found in the fcc crystalline phase if there were a random distribution of iron-iron distances around 2.54 Å.[26] It is therefore worthwhile examining the atomic structures of iron-rich Zr and Y amorphous alloys in detail to look for resemblances between the amorphous and close-packed crystalline structures.

With hydrogen, both series of alloys tend towards a common ferromagnetic state. The effect on the yttrium alloys is particularly striking, because a great change in magnetic properties is achieved with very little modification of the iron moment. It seems that the role of hydrogen is essentially to dilate the structure so as to shift the exchange distribution $P(J)$ towards increasingly positive values. The situation in the zirconium alloys is more complex because not only is the anomalously weak character of the iron magnetization altered as the moment returns to its more usual value of around $2\mu_B$, but the net exchange interaction may increase or decrease, depending on the sample. In any case, the overall result is to raise T_C above room temperature to values like those of hydrogenated *a*Fe-Y. Expanded amorphous iron would therefore seem to be a normal ferromagnet with a moment of about 2.2μ and $T_C \gtrsim 500$ K. That three limiting states for amorphous iron with very different magnetic properties can exist with rather similar energy (so similar in fact that transitions between them may occur as a function of temperature[17]) is, perhaps, not so surprising when we reflect on the differences in the magnetic properties of bcc, fcc, and hcp iron.[11]

The ability of noncrystalline alloys of iron with early transition metals (and rare earths) to absorb and retain substantial quantities of hydrogen, thereby enhancing their ferromagnetic character has implications of both theoretical and practical importance. The prospect of continuously varying the exchange in these alloys should stimulate the search for spin glass→ferromagnetic transitions at zero temperature. On the practical side, hydrogen opens up the possibility of improving the magnetic characteristics of iron-rich amorphous alloys, and of controlling the compensation temperature for ferrimagnetic and sperimagnetic rare-earth transition-metal compositions. The mechanical integrity of the amorphous hydrogenated material, in contrast to many crystalline intermetallic hydrides, will obviously be of benefit here.

ACKNOWLEDGMENTS

The authors are grateful to colleagues in the CNRS, Grenoble (D. Gignoux, A. Liénard and J. P. Rebouillat) and at McGill University, Montreal (Z. Altounian and J. O. Ström-Olsen) with whom they have collaborated on many aspects of the work. We acknowledge help received from J. Allan and E. Devlin.

[1] *Hydrogen in Metals*, edited by G. Alefeld and J. Volkl (Springer, Berlin, 1978), 2 volumes.
[2] J. H. Weaver, D. J. Peterman, and D. T. Peterson, in *Electronic Structure and Properties of Hydrogen in Metals* (Plenum, New York, 1982), p. 207.
[3] P. H. Smit, H. C. Donkersloot, and K. H. J. Buschow, J. Appl. Phys. **53**, 2640 (1982).
[4] K. H. J. Buschow and A. M. van Diepen, Solid State Commun. **19**, 79, 421 (1976).
[5] G. E. Fish, J. J. Rhyne, S. K. Sankar, and W. E. Wallace, J. Appl. Phys. **50**, 2003 (1979).
[6] K. Moorjani and J. M. D. Coey, *Magnetic Glasses* (Elsevier, Amsterdam, 1984), p. 490.
[7] R. Hasegawa and R. Roy, J. Appl. Phys. **49**, 4174 (1978); C. L. Chien and K. M. Unruh, Phys. Rev. B **24**, 1556 (1981).
[8] T. Masumoto, S. Ohnuma, K. Shirakawa, M. Nose, and K. Kobuyoshi, J. Phys. (Paris) **41**, C8–686 (1980).
[9] K. Shirakawa, K. Fukaruchi, T. Kaneko, and T. Masumot, Physica **119B**, 192 (1983).
[10] J. M. D. Coey, D. Givord, A. Liénard, and J. P. Rebouillat J. Phys. F **11**, 2707 (1981); J. Chappert, J. M. D. Coey, A. Liénard, and J. P. Rebouillat, J. Phys. F **11**, 2727 (1981).
[11] T. Kemeny, F. J. Litterst, I. Vincze, and R. Wappling, J. Phys. F **13**, L37 (1983).
[12] A. P. Malozemoff, S. R. Williams, K. Terakura, V. L. Moruzzi, and K. Fukamichi, J. Magn. Magn. Mater. (1983) (in press).
[13] K. Shirakawa, T. Kaneko, M. Nose, S. Ohnuma, H. Fujimori, and T. Masumoto, J. Appl. Phys. **52**, 1829 (1981).
[14] S. N. Kaul, Phys. Rev. B **27**, 6923 (1983).
[15] H. Fujimori, K. Nakanishi, K. Shirakawa, T. Masumoto, T. Kaneko, and N. S. Kazama, *Proceedings of the 4th International Conference on Rapidly Quenched Metals* (The Metal Society of Japan, Sendai, 1982), p. 1629; H. Fujimori, K. Nakanishi, H. Hiroyoshi, and N. S. Kazama, J. Appl. Phys. **53**, 7792 (1982).
[16] J. M. D. Coey, D. H. Ryan, D. Gignoux, A. Liénard, and J. P. Rebouillat, J. Appl. Phys. **53**, 7804 (1982).
[17] Yu Boliang, D. H. Ryan, J. M. D. Coey, Z. Altounian, J. O. Ström Olsen, and F. Razavi, J. Phys. F **13**, L217 (1983).
[18] C. G. Rabbing, Z. D. Chen, J. G. Zhao, M. J. O'Shea, and D. J. Sellmyer, J. Appl. Phys. **53**, 7798 (1982); M. Nose, Y. Moshi, T. Ishiwatari, and S. Yamanaka, J. Appl. Phys. **53**, 7807 (1982).
[19] J. P. Rebouillat (private communication).
[20] B. S. Berry and W. C. Pritchet, Phys. Rev. B **24**, 2299 (1981).
[21] G. M. Kalvius, U. F. Klein, and G. Wortmann, J. Phys. (Paris) **35**, C6–139 (1974).
[22] D. Grieg and M. A. Houson, Solid State Commun. **42**, 729 (1981).
[23] H. Hiroyoshi and K. Fukamichi, J. Appl. Phys. **53**, 2226 (1982).
[24] Y. Obi, L. C. Wang, R. Motsay, D. G. Onn, and M. Nose, J. Appl. Phys. **53**, 2304 (1982).
[25] G. Cort, R. D. Taylor, and J. O. Willis, J. Appl. Phys. **53**, 2064 (1982).
[26] W. Kummerle and U. Gradmann, Solid State Commun. **24**, 33 (1977).